Physica Scripta

PAPER

Phonon-assisted leakage current of InGaN light emitting diode

Tomas Grinys[1], **Kristupas Razas**[1], **Žydrūnas Podlipskas**[1], **Virginijus Bukauskas**[2] and **Sandra Stanionytė**[2]

[1] Institute of Photonics and Nanotechnology, Vilnius University, Sauletekio av. 3, Vilnius 10257, Lithuania
[2] Center for Physical Sciences and Technology, Sauletekio av. 3, Vilnius 10257, Lithuania

E-mail: tomas.grinys@tmi.vu.lt

Keywords: phonon, tunneling, InGaN, light-emitting diodes, dislocations

OPEN ACCESS

RECEIVED
4 October 2023

REVISED
19 July 2024

ACCEPTED FOR PUBLICATION
31 July 2024

PUBLISHED
13 August 2024

Abstract

We report on the leakage current mechanism in a blue GaN-based light-emitting diode (LED). The device structure was grown by the MOCVD technique on a sapphire substrate. The LED was characterized through various measurements including current-voltage, electroluminescence, and secondary ion mass spectroscopy (SIMS). Capacitance-voltage measurements were employed to calculate the depletion layer thickness at different bias voltages and to analyze the doping profile in the active layer. The reverse temperature-dependent current-voltage measurements were carried out to study the leakage mechanism. The leakage current was explained by phonon-assisted tunneling of charge carriers through deep trap states. The trap energy and density of states were extracted from the application of the introduced model. Cathodoluminescence measurements were performed to evaluate the density of dislocations, which were then compared to x-ray diffraction measurements. The determined value was close to the density of states obtained from the tunneling model.

1. Introduction

GaN-based materials are III/V group direct bandgap semiconductors used in optoelectronic devices, such as light-emitting diodes (LEDs). Studies on the leakage current mechanism of these devices are of particular importance due to their immense potential to further increase reliability and energy efficiency, especially when reducing the size of the devices. GaN technology still faces a problem: the absence of cost-effective bulk substrates for homoepitaxy. Most of the GaN layer growth is conducted on thermal coefficient and lattice-mismatched substrates such as sapphire, silicon, or SiC [1]. This leads to the presence of imperfections inside the crystal including extended defects such as various types of dislocations. The extended defects, particularly threading dislocations, can propagate throughout the entire structure of the device, creating spatially closed defect states [2]. These defects are responsible for the leakage current in the space charge region of the p–n junction [3]. Studies show that the carrier transport mechanism is dominated by tunneling through the deep defect states within the band gap. Reverse [4–7] or low current direct [8, 9] temperature-dependent current-voltage measurements are usually performed to analyze the leakage mechanism.

Recently, various attempts have been made to model reverse leakage currents in GaN-based structures, employing mechanisms such as the Pool-Frenkel effect and trap-assisted tunneling [10, 11]. However, these models exhibit limitations in the two key areas: matching experimental data across a wide temperature range, and establishing a strong relationship between the extracted parameters and the crystalline quality of GaN-based materials.

In contrast, the phonon-assisted tunneling model, introduced by P. Pipinys *et al* [12], has demonstrated good agreement with the reverse current-voltage characteristics of the nGaN Schottky diode structure across a wide temperature range. Efforts have also been made to apply this model for the explanation leakage currents in high mobility transistors (HEMTs) [13]. In our current study, we investigate the applicability of this model to a more complex LED device structure. We conduct a detailed current-voltage, electro-luminescence characterization of the as-grown LED device. The second ion mass spectroscopy (SIMS) and

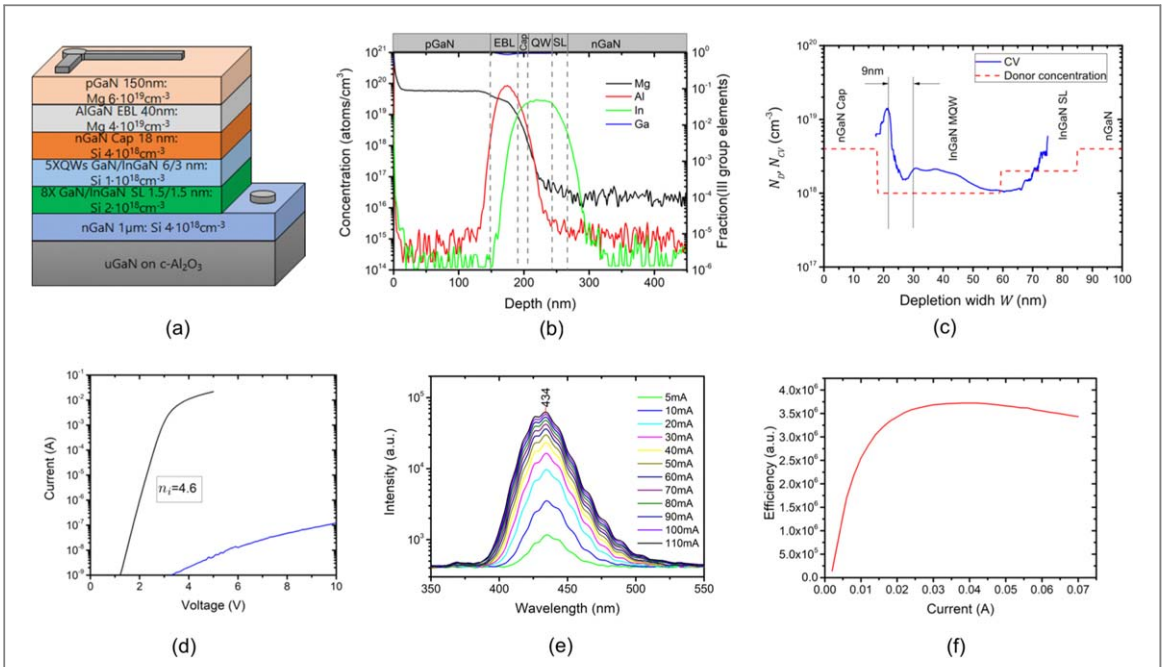

Figure 1. Blue InGaN LED characteristics. Structure of grown LED device (a). Mg dopant and III group element concentration profile determined by SIMS. Dashed curves indicate the boundaries of corresponding layers (b). Concentration N_{CV} extracted from CV profile measured at room temperature (solid curve). The dashed curve shows the Si donor concentration N_D injected during MOCVD growth (c). Forward and reverse current-voltage curves (d). Electroluminescence at different injection currents (e). Efficiency as a function of current (f).

capacitance-voltage (CV) measurements we performed to analyze the doping concentration, focusing on the active layer of LED. We have demonstrated that the density of defect states extracted from reverse current-voltage characteristics at different temperatures can be directly related to the density of threading dislocations. The threading dislocation density was measured by means of cathodoluminescence and further validated through XRD analysis in the current paper.

2. Experimental

The metal face III-nitride epitaxial layers of the LED were grown on a c-plane sapphire substrate using an AIXTRON (3x2) metal-organic chemical vapor deposition (MOCVD) reactor. The mesa structures were fabricated through photolithography using laser writing equipment, followed by inductively coupled plasma reactive ion etching (ICP-RIE) from Oxford Instruments. A gas mixture of Ar/Cl_2 was used for dry etching at a rate of 5 nm/s. The ICP-RIE etched profile exhibits a steepness of around 75°. To remove native oxide and to minimize current leakage caused by surface imperfections after RIE, we performed an HF acid treatment on the structures. For the contacts, we utilized e-beam-evaporated Ni/Au and Ti/Au metals for Mg-doped p-type and Si-doped n-type GaN, respectively. The mesas of devices had dimensions of $270 \times 270\ \mu m^2$. The structure of the LED cross-section is depicted in figure 1(a) and consists of an n-type GaN layer, an eight-period GaN/InGaN superlattice (SL), a five-period GaN/InGaN multiple quantum wells (MQW), an n-type GaN cap layer, an AlGaN electron-blocking layer, and is finished with a p-type GaN layer. The p-type Mg dopant, as well as the distribution profile of III group elements determined by secondary ion mass spectroscopy (SIMS) is shown in figure 1(b). The distribution of donor concentration N_D in the vicinity of the MQW active layer evaluated from the flows of the MOCVD process is illustrated in figure 1(c) for comparison with the corresponding capacitance-voltage (CV) measurement results. The CV characterization was achieved using Keithley 4200-CVU module, integrated within the Keithley 4200-SCS Semiconductor Characterization System. Cathodoluminescence images were taken at room temperature with an acceleration voltage set to 4 kV. Depending on the magnification, the e-beam was scanned in steps of 14-to-46 nm with a dwell time set to 1 ms. Automatic defect/dislocation identification was performed using a custom Python code and the Laplacian of Gaussian Blob Detection algorithm from scikit-image library [14]. Additionally, the x-ray diffraction method (XRD) with a Cu Kα radiation source was used to evaluate the screw-type dislocation density and to confirm the cathodoluminescence measurement results.

3. Results and discussion

3.1. Characterization of LED device

The LED for studying leakage mechanisms was fabricated with an additional embedded Si-doped GaN layer on top of the multiple quantum well (MQW) structure. This layer affects the band structure of the device by shifting the MQW region towards the n-type side of the junction, resulting in a more abrupt p–n junction. The electric field distribution in the space charge region of such an LED structure is similar to that of a GaN p–n junction without the MQW.

Figure 1(d) presents the forward and reverse current-voltage characteristics of the LED measured at room temperature, plotted in semi-log scale. The device exhibits good rectifying behaviour, with a reverse leakage current as low as 10^{-7} A at 10 V. The forward current-voltage curve is linear in semi-log scale up to 3 V. The dependence in this region can be described by Shockley's diode equation: $I = I_0 \exp(qV/(n_i k_B T))$, where I_0 is the pre-exponential factor, q is the elementary charge, V is the bias voltage, n_i is the ideality factor, k_B is the Boltzmann constant, and T is the absolute temperature. According to this equation, it was found that $n_i = 4.6$. An ideality factor larger than 2 is a criterion for dominating tunneling in the charge transport mechanism.

Figure 1(e) displays the electroluminescence measurement spectra at different injection currents. The peak maximum of the emitted light is at a wavelength of 434 nm, and it remains stable over the entire measured current range. This stability can be attributed to the design of the LED, which minimizes the impact of changes in the built-in potential on the energy levels of the states within the multiple quantum wells (MQWs) when forward current is applied. The ratio of light emission power to electrical power, or LED efficiency, versus injection current is presented in figure 1(f). The LED efficiency increases up to 30 mA, after which the efficiency droop effect is observed. This phenomenon is typical for LED devices [15].

3.2. CV measurement analysis

The CV measurements were performed at 1 MHz using an altering current signal level of 15 mV under ambient conditions at room temperature. The dopant concentration can be calculated by the following equation:

$$N_{CV} = \frac{2}{q\varepsilon\varepsilon_0 A^2 d(1/C^2)/dV} \tag{1}$$

where ε and ε_0 are relative and absolute dielectric constants, respectively. A is the area of the device, C is the measured capacitance at corresponding bias voltage V. The depletion width W is related to capacitance as $W = \varepsilon\varepsilon_0 A/C$. By employing the equations mentioned above, the dopant concentration profiles can be determined. Figure 1(c) displays the solid curve, which represents the CV profile plot of the LED. Periodic damping peaks are observed in the MQWs region, and the distance between these peaks is approximately 9 nm, corresponding to the period of the MQWs [4, 16]. Additionally, some periodic steps can be identified in the adjacent InGaN SL region, which is close to the periodicity 3 nm of the SL structure.

The acceptor level of Mg is deep within a band gap, it can make complexes with hydrogen during MOCVD growth and suffers from self-compensation effect [17, 18]. A high number of Mg atoms are needed to reach sufficient conductivity. However, when a p–n junction is formed especially in a reverse bias regime the band bending occurs. This effect results in a change in the ionization state of Mg and leads to a high ionized acceptor concentration in the depletion region [19]. Therefore, the p–n junction is highly asymmetric in GaN-based material with the depletion region penetrating into the n-side of the junction. This situation is shown in figure 2 where modeled n-side and total depletion width curves are close to each other.

The total depletion width can be evaluated by the following equation:

$$W = \sqrt{\frac{2\varepsilon\varepsilon_0}{q}(V_0 - V)\left(\frac{1}{N_A} + \frac{1}{N_D}\right)} \tag{2}$$

where built-in voltage (V_0) is equal to 3.3 V, and V is the applied reverse bias voltage. At zero bias, the depletion width is approximately 30 nm. The curves shown in figure 2 were modeled with donor and acceptor concentrations at values $N_D = 2 \cdot 10^{18}$ cm^{-3} and $N_A = 4 \cdot 10^{19}$ cm^{-3}, respectively. The N_D value corresponds to the average donor concentration obtained from CV dopant profile above a depletion width of 30 nm (figure 1(c)). Additionally, the N_A value is attributed to the average Mg dopant concentration in the p-type electron blocking layer determined from SIMS analysis (figure 1(e)). The curve extracted from CV measurements (figure 2) demonstrates good agreement with the calculated total depletion width values above the reverse voltage of 5 V. However, in the low voltage range, the CV curve falls below the modeled values. To achieve a better fit with the CV curve in the low voltage range, the dopant concentration N_D should be increased to around $3{\cdot}10^{18}$ cm^{-3}, considering that the depletion width (equation (2)) is inversely proportional to the dopant concentration. The increased dopant concentration in the low voltage range coincides with the CV profile rather than the Si dopant profile (see figure 1). It should be emphasized, that the indium concentration is

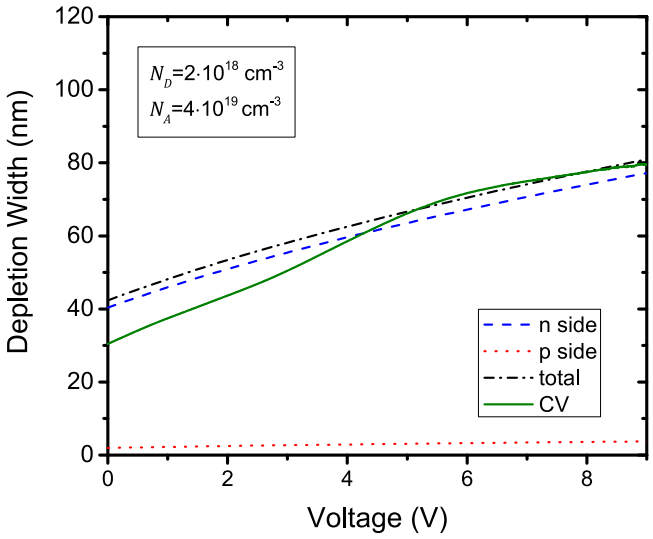

Figure 2. Depletion width dependence on the applied voltage. The solid curve represents CV measurements. Dash-dotted, dashed, and dotted curves show modeled results with corresponding donor and acceptor concentrations.

higher in the InGaN solid solution of the MQW compared to the SL of the produced LED. The indium-induced defects can contribute to the higher N_{CV} concentration observed in the MQW region.

3.3. Interpretation of reverse leakage current

Numerous studies on the reverse leakage current of LEDs demonstrate that a high amount of energy is required to excite trapped charge carriers from states within the band gap. This conduction mechanism can be explained by multi-step tunneling through these deep states. In such a case, the leakage current I is directly proportional to the number of states N_s and the tunneling rate P:

$$I = qAN_sP \tag{3}$$

For phonon-assisted charge carrier tunneling, the rate depends on temperature T and electric field E. If the tunneling process occurs through a triangular barrier of depth ε_T, the tunneling rate can be described as [12]:

$$\begin{aligned} P = {} & \frac{eE}{(8m^*\varepsilon_T)^{1/2}}[(1+\gamma^2)^{1/2}-\gamma]^{1/2}[1+\gamma^2]^{-1/4} \\ & \times exp\left\{-\frac{4}{3}\frac{(2m^*)^{1/2}}{eE\hbar}\varepsilon_T^{3/2}[(1+\gamma^2)^{1/2}-\gamma]^2 \right. \\ & \left. \times \left[(1+\gamma^2)^{1/2}+\frac{1}{2}\gamma\right]\right\} \end{aligned} \tag{4}$$

where

$$\gamma = \frac{(2m^*)^{1/2}\Gamma^2}{8e\hbar E\varepsilon_T^{1/2}} \tag{5}$$

The $\Gamma = 8a(\hbar\omega)^2(2n+1)$ represents the width of the center absorption band with a phonon distribution function $n = [exp(\hbar\omega)/(k_BT) - 1]^{-1}$. The parameter a is a charge carrier-phonon interaction constant, and $\hbar\omega$ is phonon energy.

The average electric field in the depletion region of the LED can be evaluated using $E = (V_0 - V)/W$. By substituting equation (2) into the electric field expression, one can obtain that the average internal electric field is proportional to the square root of the total electrostatic potential, i.e., $E \sim \sqrt{(V_0 - V)}$. This relationship, along with the proportionality constant that includes donor and acceptor concentration values given in the inset of figure 2, was incorporated into the tunneling model to fit the experimental measurements. Figure 3 displays the current-voltage characteristics along with the modeling results at different temperatures. Two main parameters, trap energy, and density of states were varied to obtain the best fitting results. We found that trap energy can be as high as 0.89 ± 0.01 eV, while density of states is equal to 4.6·10^8 ± 1.6·10^8 cm^{-2}. The other parameters remained the same as in [12], except for the effective mass. Unlike the Schottky diode analyzed in [12], the LEDs contain GaN/AlGaN heterostructures. Therefore, the effective mass of electrons can be as high as 0.4m_e [20, 21].

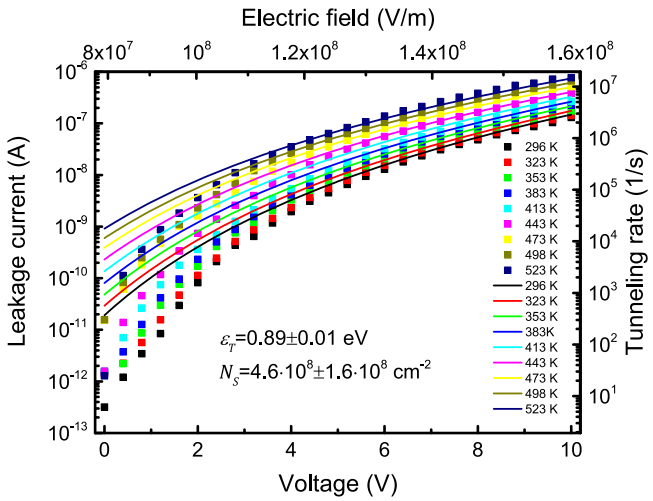

Figure 3. Temperature dependent reverse current-voltage characteristics. Dots represent experimental measurements, while solid curves model results. Parameters such as effective mass $m^* = 0.4m_e$, electron-phonon interaction constant $a = 2$, optical phonon energy $\hbar\omega = 0.07$ eV were chosen to fit the trap energy ε_T and density of occupied states N_s.

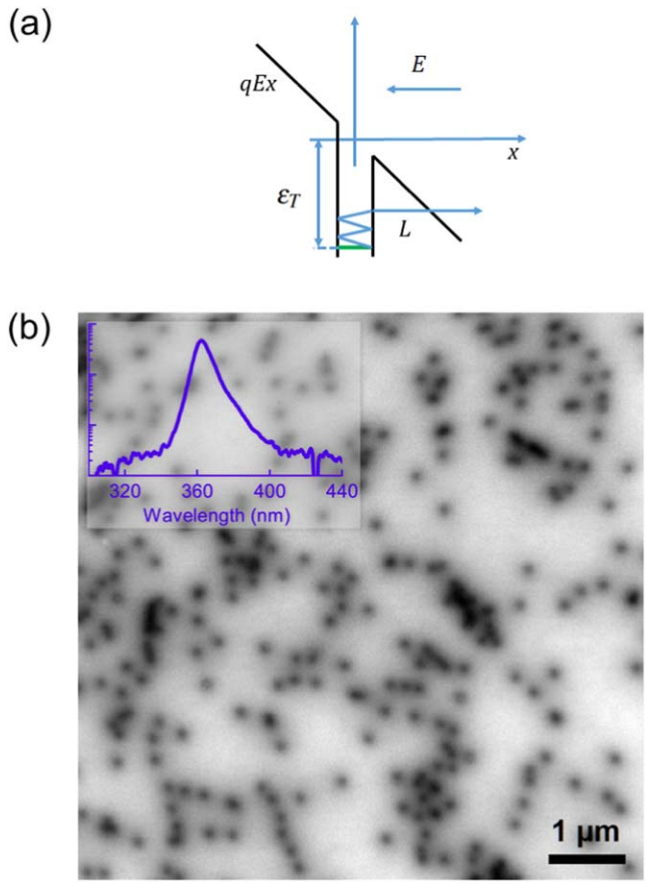

Figure 4. Schematic diagram of phonon-assisted tunneling phenomena (a). The cathodoluminescence intensity map excited with 4 keV electrons in the nGaN layer of the LED and measured at a wavelength of 363 nm; the inset shows the spatially averaged cathodoluminescence spectrum.

Figure 3 demonstrates that the phonon-assisted tunneling model does not fit the experimental data well below 5 V. When using the depletion width values extracted from CV measurements and substituting them into the model, there is an even higher deviation in the low voltage range. For the triangular tunneling barrier depicted in figure 4(a), the tunneling length L can be determined using the relationship $qEL = \varepsilon_T C_\gamma^{2/3}$, where $C_\gamma^{2/3}$ represents the term with variables γ inside the exponent of equation (4). The calculated tunneling length

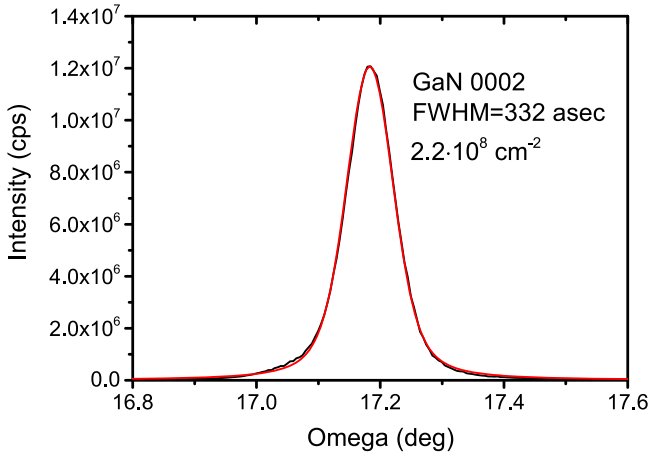

Figure 5. Rocking curve scan of GaN(0002) reflection. Red curve shows fitting to Voigt function.

values, obtained from this relationship, vary from 5.3 nm to 4.5 nm in the range of 5-10 V at room temperature. These values are reasonable for the tunneling process. However, the high tunneling length at a lower bias voltage can lead to a deviation from the presented model.

Figure 4(b) shows the cathodoluminescence (CL) intensity distribution map with a peak wavelength of 363 nm. This photon emission wavelength corresponds to the direct band gap charge carrier recombination process in GaN. The CL mapping was obtained in the area of the RIE-etched LED, reaching the nGaN layer close to the exact device under investigation. Dislocation defects in GaN are active non-radiative recombination centers, resulting in the reduced intensity of CL. To quantify the dislocation density, we performed a numerical analysis of the CL image, identifying the number of dark areas. Consequently, the average number of dislocations was found to be $4.3{\cdot}10^8 \pm 2.7{\cdot}10^8$ cm^{-2}, a value very close to the density of states determined by the phonon-assisted tunneling model.

High-resolution XRD analysis of the LED structure is shown in figure 5. The XRD rocking curve measurement of reflection from the GaN(0002) lattice plane revealed a full width at half maximum (FWHM) equal to 332 arcseconds. According to the model proposed by Dunn and Koch [22], the density of screw-type threading dislocations can be calculated using the equation $\varrho = \beta^2/(4.36b^2)$, where β is the peak broadening and b is the magnitude of the Burgers vector. This model gives a screw-type threading dislocation density value of $\varrho = 2.2 \cdot 10^8$ cm^{-2}. This value is in the same order of magnitude, although about half, of the threading dislocation density determined by cathodoluminescence. The observed mismatch may be due to measurements of slightly different locations on the same wafer. Additionally, some other technical factors such as probing depth, that come from the origin of these two methods can lead to the difference observed [23].

4. Conclusions

In summary, we analyzed the CV measurements and IV characteristics of GaN-based LED with a peak wavelength at 434 nm. We employed a phonon-assisted tunneling model to fit the reverse IV experimental data in the temperature range 296-523 K. The model showed good fitting results at a higher bias voltage above 5V. The tunneling occurs from the deep-state traps of energy 0.89 eV, which are responsible for the internal leakage current. Our findings revealed, that the density of states ($4.6{\cdot}10^8$ cm^{-2}) shows good agreement with the number of dislocations ($4.3{\cdot}10^8$ cm^{-2} from CL measurements and $2.2{\cdot}10^8$ cm^{-2} from XRD analysis). The formation of dislocations during the epitaxy of LED leads to a higher density of deep traps.

Acknowledgments

This research was funded by the Research Council of Lithuania under grant agreement no. S-MIP-23-42.

Data availability statement

All data that support the findings of this study are included within the article (and any supplementary files).

ORCID iDs

Tomas Grinys https://orcid.org/0000-0002-5725-1092
Virginijus Bukauskas https://orcid.org/0000-0003-0275-9603
Sandra Stanionytė https://orcid.org/0000-0003-0018-5036

References

[1] Lee M, Lee H U, Song K M and Kim J 2019 Significant improvement of reverse leakage current characteristics of Si-based homoepitaxial InGaN/GaN blue light emitting diodes *Sci. Rep.* **9** 970
[2] Monemar B and Sernelius B 2007 Defect related issues in the 'current roll-off' in InGaN based light emitting diodes *Appl. Phys. Lett.* **91** 181103
[3] Narita T *et al* 2022 Identification of type of threading dislocation causing reverse leakage in GaN p-n junctions after continuous forward current stress *Sci. Rep.* **12** 1458
[4] Shan Q, Meyaard D S, Dai Q, Cho J, Fred Schubert E, Kon Son J and Sone C 2011 Transport-mechanism analysis of the reverse leakage current in GaInN light-emitting diodes *Appl. Phys. Lett.* **99** 253506
[5] Jung E, Lee J K, Kim M S and Kim H 2015 Leakage current analysis of GaN-based light-emitting diodes using a parasitic diode model *IEEE Trans. Electron Devices* **62** 3322–5
[6] Kim J, Kim J, Tak Y, Chae S, Kim J Y and Park Y 2013 Effect of v-shaped pit size on the reverse leakage current of InGaN/GaN light-emitting diodes *IEEE Electron Device Lett.* **34** 1409–11
[7] Zhou S, Lv J, Wu Y, Zhang Y, Zheng C and Liu S 2018 Reverse leakage current characteristics of InGaN/GaN multiple quantum well ultraviolet/blue/green light-emitting diodes *Japan. J. Appl. Phys.* **57** 051003
[8] Yan D, Lu H, Chen D, Zhang R and Zheng Y 2010 Forward tunneling current in GaN-based blue light-emitting diodes *Appl. Phys. Lett.* **96** 083504
[9] Roccato N *et al* 2021 Modeling the electrical characteristics of InGaN/GaN led structures based on experimentally-measured defect characteristics *J. Phys. D: Appl. Phys.* **54** 425105
[10] Li S, Ercan B, Ren C, Ikeda H and Chowdhury S 2022 A study on the impact of dislocation density on leakage current in vertical GaN-on-GaN p-n diodes *IEEE Trans. Electron Devices* **69** 4206–11
[11] Jiang X, Li C H, Yang S X, Liang J H, Lai L K, Dong Q Y, Huang W, Liu X Y and Luo W J 2023 Reverse gate leakage mechanism of AlGaN/GaN HEMTs with Au-free gate *Chin. Phys.* B **32** 037201
[12] Pipinys P and Lapeika V 2006 Temperature dependence of reverse-bias leakage current in GaN schottky diodes as a consequence of phonon-assisted tunneling *J. Appl. Phys.* **99** 093709
[13] Mukherjee J, Chaubey R K, Rawal D and Dhaka R 2022 Analysis of the post-stress recovery of reverse leakage current in GaN HEMTs *Mater. Sci. Semicond. Process.* **137** 106222
[14] Nunez-Iglesias J 2023 (https://scikit-image.org/docs/stable/api/skimage.feature.html)
[15] Schubert M F, Chhajed S, Kim J K, Schubert E F, Koleske D D, Crawford M H, Lee S R, Fischer A J, Thaler G and Banas M A 2007 Effect of dislocation density on efficiency droop in GaInN/GaN light-emitting diodes *Appl. Phys. Lett.* **91** 231114
[16] Chen N, Lien W, Wang Y and Liu H 2007 Capacitance-voltage and current-voltage measurements of nitride light-emitting diodes *IEEE Trans. Electron Devices* **54** 3223–8
[17] Brochen S, Brault J, Chenot S, Dussaigne A, Leroux M and Damilano B 2013 Dependence of the Mg-related acceptor ionization energy with the acceptor concentration in p-type GaN layers grown by molecular beam epitaxy *Appl. Phys. Lett.* **103** 269904
[18] Castiglia A, Carlin J F and Grandjean N 2011 Role of stable and metastable Mg-H complexes in p-type GaN for cw blue laser diodes *Appl. Phys. Lett.* **98** 213505
[19] Wierer J J, Dickerson J R, Allerman A A, Armstrong A M, Crawford M H and Kaplar R J 2017 Simulations of junction termination extensions in vertical GaN power diodes *IEEE Trans. Electron Devices* **64** 2291–7
[20] Burmistrov E and Avakyants L 2021 The relaxation time, mobility, and effective mass of 2DEG in InGaN/GaN quantum wells according to terahertz plasmon resonance data *Moscow Univ. Phys. Bull.* **76** 371–9
[21] Pashnev D, Korotyeyev V V, Jorudas J, Urbanowicz A, Prystawko P, Janonis V and Kašalynas I 2022 Investigation of electron effective mass in AlGaN/GaN heterostructures by THz spectroscopy of drude conductivity *IEEE Trans. Electron Devices* **69** 3636–40
[22] Dunn C and Kogh E 1957 Comparison of dislocation densities of primary and secondary recrystallization grains of Si-Fe *Acta Metall.* **5** 548–54
[23] Yon V, Rochat N, Charles M, Nolot E and Gergaud P 2020 X-ray diffraction microstrain analysis for extraction of threading dislocation density of GaN films grown on silicon, sapphire, and SiC substrates *Physica Status Solidi (b)* **257** 1900579